

Electronic and magnetic structures of ternary iron selenides $A\text{Fe}_2\text{Se}_2$ ($A=\text{K}$, Cs , or Tl)

Xun-Wang Yan^{1,2}, Miao Gao¹, Zhong-Yi Lu^{1,*} and Tao Xiang^{3,2†}

¹*Department of Physics, Renmin University of China, Beijing 100872, China*

²*Institute of Theoretical Physics, Chinese Academy of Sciences, Beijing 100190, China and*

³*Institute of Physics, Chinese Academy of Sciences, Beijing 100190, China*

(Dated: November 9, 2018)

By the first-principles electronic structure calculations, we find that the ground state of ternary iron selenides $A\text{Fe}_2\text{Se}_2$ ($A=\text{K}$, Cs , or Tl) is in a bi-collinear antiferromagnetic order, in which the Fe local moments ($\sim 2.8\mu_B$) align ferromagnetically along a diagonal direction and antiferromagnetically along the other diagonal direction on the Fe-Fe square lattice. This bi-collinear antiferromagnetic order results from the interplay among the nearest, the next nearest, and the next next nearest neighbor superexchange interactions, mediated by Se $4p$ -orbitals.

PACS numbers: 74.25.Jb, 71.18.+y, 74.70.-b, 74.25.Ha, 71.20.-b

The discovery of high transition temperature T_c superconductivity in LaFeAsO by partial substitution of O with F atoms [1] stimulates the intense studies on the iron pnictides. There have been four types of iron-based compounds reported to show superconductivity after doping or under high pressures, i.e. 1111-type ReFeAsO (Re = rare earth) [1], 122-type BFe_2As_2 ($B=\text{Ba}$, Sr , or Ca) [2], 111-type AFeAs (A = alkali metal) [3], and 11-type tetragonal $\alpha\text{-FeSe}(\text{Te})$ [4]. It was very recently reported that the superconductivity was observed at about 30 K in a new FeSe-layer compound $\text{K}_{0.8}\text{Fe}_2\text{Se}_2$ [5], formed by intercalating potassium (K) atoms between FeSe layers. Soon after, the superconductivity was also found in the Cs-intercalated compound $\text{Cs}_{0.8}(\text{FeSe}_{0.98})_2$ [6] and Tl-intercalated compound TlFe_xSe_2 [7]. Although these the compounds take the ThCr_2Si_2 type structure with $P4/nmm$ symmetry isostructural with 122-type BFe_2As_2 , they can be considered as a new type of iron-based superconductors since they are chalcogenides rather than pnictides.

For the parent compounds $A\text{Fe}_2\text{Se}_2$ ($A=\text{K}$, Cs , or Tl) of these new superconductors, the intercalated alkali metal or Tl atoms will directly dope much more electrons into the FeSe layers than for the iron pnictides. It is thus expected that the electronic and magnetic structures of these new compounds are very likely different from the ones of those iron pnictides. On the other hand, in order to investigate the mechanism of superconductivity in these materials, one needs to first understand the electronic and magnetic structures of the parent compounds $A\text{Fe}_2\text{Se}_2$.

In this paper, we report the theoretical result on the electronic and magnetic structures of iron selenides $A\text{Fe}_2\text{Se}_2$ ($A=\text{K}$, Cs , or Tl) obtained from the first-principles electronic structure calculations. We find that the compounds $A\text{Fe}_2\text{Se}_2$ are antiferromagnetic semimetals with a bi-collinear antiferromagnetic order in the ground states, resulting from the strong nearest (J_1), next-nearest (J_2), and next-next-nearest (J_3) neighbor superexchange interactions in these materials. A small

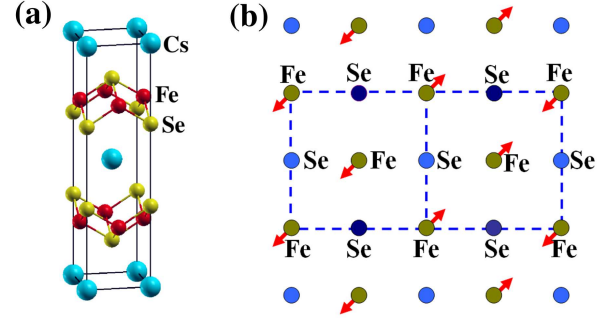


FIG. 1: (Color online) CsFe_2Se_2 with the ZrCuSiAs -type structure: (a) a tetragonal unit cell containing two formula units; (b) schematic top view of the FeSe layer. The large dashed square is a $a \times 2a$ unit cell. The Fe spins in the bi-collinear antiferromagnetic order are shown by the red arrows.

monoclinic lattice distortion due to spin-lattice coupling was further found in these compounds, similar to $\alpha\text{-FeTe}$ [8, 9]. Here the bi-collinear antiferromagnetic (AFM) order means that the Fe moments align ferromagnetically along a diagonal direction and antiferromagnetically along the other diagonal direction on the Fe-Fe square lattice. In other words, if the Fe-Fe square lattice is divided into two square sublattices, the Fe moments on each sublattice take their own collinear AFM order. The bi-collinear antiferromagnetic order was first predicted for $\alpha\text{-FeTe}$ by our previous work [8] and confirmed by the later neutron scattering experiment [9].

Although $A\text{Fe}_2\text{Se}_2$ can be considered as a tetragonal crystal with two formula units included in the corresponding unit cell as shown in Fig.1(a), its primitive unit cell is constructed by considering $A\text{Fe}_2\text{Se}_2$ as a triclinic crystal, in which only one formula unit cell is included. In the nonmagnetic calculations, we adopted the primitive cell as a calculation cell. In the calculation of the electronic and magnetic structures of the ferromagnetic and the square antiferromagnetic Neel states, the $a \times a$ FeSe cell is taken as the base cell. In the calculation of the

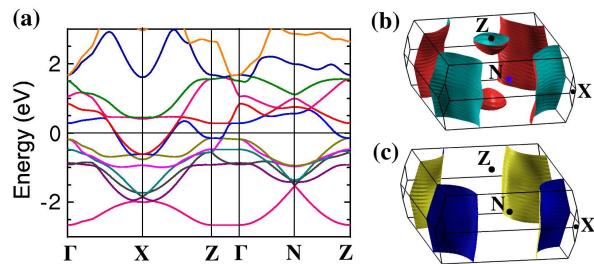


FIG. 2: (Color online) CsFe₂Se₂ in the nonmagnetic state: (a) energy band structure; (b) the Fermi surface sheets due to the band crossing the Fermi energy marked by the blue line in the left figure; (c) the Fermi surface sheet due to the band crossing the Fermi energy marked by the red line in the left figure.

collinear and bi-collinear antiferromagnetic states, the unit cells are doubled and the base cells are the $\sqrt{2}a \times \sqrt{2}a$ and $a \times 2a$ (Fig. 1 (b)) FeSe cells, respectively.

In our calculations the plane wave basis method was used [10]. We adopted the generalized gradient approximation (GGA) of Perdew-Burke-Ernzerhof [11] for the exchange-correlation potentials. The ultrasoft pseudopotentials [12] were used to model the electron-ion interactions. After the full convergence test, the kinetic energy cut-off and the charge density cut-off of the plane wave basis were chosen to be 800 eV and 6400 eV, respectively. The Gaussian broadening technique was used and a mesh of $18 \times 18 \times 9$ k-points were sampled for the Brillouin-zone integration. In the calculations, the experimental tetragonal lattice parameters were adopted [5, 6], and the internal atomic coordinates within the cell were determined by the energy minimization. Actually, the lattice parameters optimized by the energy minimization in our magnetic calculations are found in excellent agreement with the experimental ones.

In Fig. 2 we plot the electronic band structure and Fermi surface of CsFe₂Se₂ in the nonmagnetic state, similar to the ones just reported for KFe₂Se₂ [13]. As we see, there are three Fermi surface sheets, among which the two cylinder-like ones are located around the corners of the Brillouin zone, and another one is of small pocket. The Fermi surface is all of electron-type. The volume enclosed by these Fermi sheets give 1.008 electrons per formula cell. i.e. about $0.84 \times 10^{22}/\text{cm}^3$. The density of states (DOS) at the Fermi energy is about 2.27 states per eV per formula unit. The corresponding electronic specific heat coefficient and Pauli susceptibility are $\gamma = 5.35 \text{ mJ}/(\text{K}^2 * \text{mol})$ and $\chi = 0.92 \times 10^{-9} \text{ m}^3/\text{mol}$, respectively. Our calculations for the nonmagnetic states exclude any possible structural distortions. This suggests that any possible structural distortion happening in CsFe₂Se₂ would be driven through spin-phonon interactions. For KFe₂Se₂, the almost same results are found by our calculations.

In order to explore the magnetic structure of CsFe₂Se₂, we have calculated four different possible magnetic states with ferromagnetic, square Neel AFM, collinear AFM, and bi-collinear AFM orders, respectively. If the energy of the nonmagnetic state is set to zero, we find that the energies of the ferromagnetic (E_{FE}), square Neel AFM (E_{AFM}), collinear AFM (E_{COL}), and bi-collinear AFM states (E_{BI}) are (-0.2122, -0.1651, -0.2677, -0.2752) eV/Fe for CsFe₂Se₂ and (-0.2437, -0.1544, -0.2613, -0.2884) eV/Fe for KFe₂Se₂, respectively. Thus the ground states of both CsFe₂Se₂ and KFe₂Se₂ are in the bi-collinear antiferromagnetic order, similar to the one of α -FeTe [8]. The magnetic moment around each Fe atom is found to be about $2.4 \sim 3.0 \mu_B$, varying weakly in the above four magnetically ordered states, similar as in LaFeAsO and BaFe₂As₂ [14, 15]. Since these local moments are embedded in the environment of itinerant electrons, the moment of Fe ions is thus fluctuating.

To quantify the magnetic interactions, we assume that the energy differences between these magnetic orderings are predominantly contributed from the exchange interactions between the Fe moments with spin \vec{S}_i , which can be effectively modeled by the following frustrated Heisenberg model with the nearest, next-nearest, and next next nearest neighbor couplings J_1 , J_2 , and J_3 ,

$$H = J_1 \sum_{\langle ij \rangle} \vec{S}_i \cdot \vec{S}_j + J_2 \sum_{\langle\langle ij \rangle\rangle} \vec{S}_i \cdot \vec{S}_j + J_3 \sum_{\langle\langle\langle ij \rangle\rangle\rangle} \vec{S}_i \cdot \vec{S}_j, \quad (1)$$

whereas $\langle ij \rangle$, $\langle\langle ij \rangle\rangle$ and $\langle\langle\langle ij \rangle\rangle\rangle$ denote the summation over the nearest, next-nearest, and next-next-nearest neighbors, respectively. This model may miss certain contributions from itinerant electrons, however, we believe that it captures the substantial physics on the magnetic structures. From the above calculated energy data, we find that for CsFe₂Se₂ $J_1 = -11.78 \text{ meV}/S^2$, $J_2 = 19.75 \text{ meV}/S^2$, and $J_3 = 11.75 \text{ meV}/S^2$, while for KFe₂Se₂ $J_1 = -22.3 \text{ meV}/S^2$, $J_2 = 15.6 \text{ meV}/S^2$, and $J_3 = 14.6 \text{ meV}/S^2$ (The detailed calculation is referred to Appendix of Ref. 14). Notice that the ferromagnetic states in both the compounds are lower in energy than the square Neel AFM state, which results in the negative J_1 here.

It is known that when $J_3 > J_2/2$ and $J_2 > J_1/2$, the bi-collinear AFM state is lower in energy than the collinear AFM state for a frustrated J_1 - J_2 - J_3 Heisenberg model. This is in well agreement with the derived J_1 , J_2 , and J_3 for both CsFe₂Se₂ and KFe₂Se₂. Accordingly, by J_1 - J_2 - J_3 Heisenberg model we may understand the complex magnetic structures displayed in both the compounds. On the other hand, the classical study of J_1 - J_2 - J_3 Heisenberg model [16, 17] shows that there may be an incommensurate AFM spin order easily developed in such J_1 - J_2 - J_3 system. However, it can be shown that a slight structural distortion making J_1 different along different direction will eliminate such an incommensurate spin order [17].

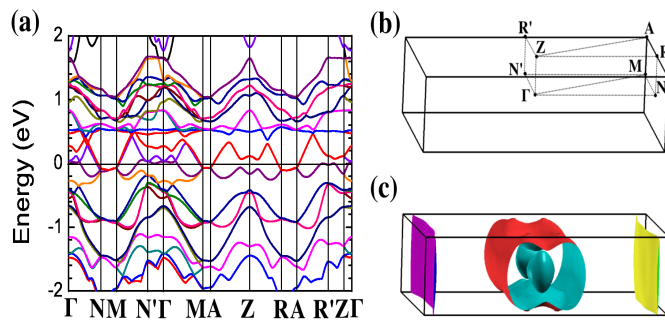


FIG. 3: (Color online) (a) Electronic band structure of CsFe_2Se_2 in the bi-collinear-ordered antiferromagnetic state. The Fermi energy is set to zero. (b) Brillouin zone. (c) Fermi surface. Notice that $\Gamma\text{-N}(\Gamma\text{-N}')$ corresponds the parallel(antiparallel)-aligned moment line.

It is expected that there would be a further lattice distortion considering possible spin-phonon interactions. Similarly to spin-Peierls distortion, the lattice constant slightly expands along spin anti-parallel alignment to lower AFM energy and/or slightly contracts along spin-parallel alignment to lower ferromagnetic energy. Indeed such small structural distortions are found for both CsFe_2Se_2 and KFe_2Se_2 with an extra energy gain of ~ 4 meV/Fe. As a result, the crystal unit cell of the compounds on FeSe layer deforms from a square to a rectangle (rhombus). Such small lattice distortions affect weakly the electronic band structures and the Fe moments.

Our calculations also show that for both CsFe_2Se_2 and KFe_2Se_2 the Fe magnetic moments between the nearest neighbor layers FeSe prefer the parallel alignment with a small energy gain of about 2 meV/Fe in comparison with the anti-parallel alignment. This is different from the iron pnictides [8, 14, 15]. It is thus very likely that here the magnetic phase transition would happen simultaneously with the structural transition. Overall the magnetic order vector in these two compounds is thus $(\frac{\pi}{a}, 0, 0)$. The corresponding magnetic Bragg peaks are $(1, 0, 0)$.

Fig. 3 shows the electronic structure of CsFe_2Se_2 in the bi-collinear AFM state, and the similar finding is for KFe_2Se_2 . There are three bands crossing the Fermi level which form four sheets of the Fermi surface. The Fermi surface contains two hole-type sheets parallel to the plane $\Gamma\text{-Z-R}'\text{-N}'$, and two electron-type cylinders parallel to the plane A-M-N-R . From the volumes enclosed by these Fermi surface sheets, we find that the electron (hole) carrier density is 0.052 electron/formula cell (0.061 hole/formula cell), namely, $0.88 \times 10^{21}/\text{cm}^3$ ($1.00 \times 10^{21}/\text{cm}^3$). The density of states (DOS) at the Fermi level E_F is 6.24 states per eV per formula cell. The corresponding electronic specific heat coefficient $\gamma = 7.34$ mJ/(K² * mol).

By projecting the density of states onto the five $3d$

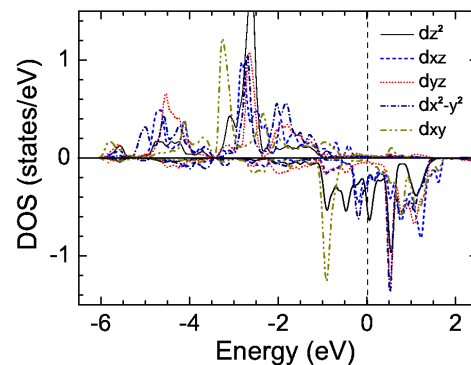


FIG. 4: (Color online) Calculated total and projected density of states at the five Fe- $3d$ orbitals around one of the four Fe atoms in the bi-collinear antiferromagnetic state unit cell of CsFe_2Se_2 . The Fermi energy is set to zero.

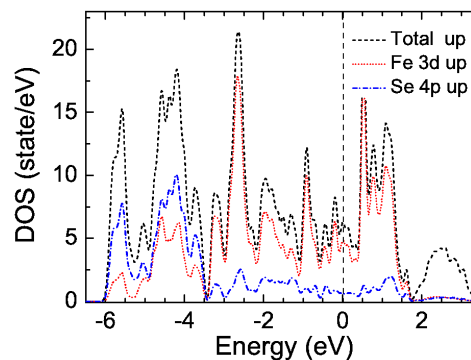


FIG. 5: (Color online) Total and orbital-resolved partial density of states (spin-up part) per four formula cells of CsFe_2Se_2 in the bi-collinear antiferromagnetic state. The Fermi energy is set to zero.

orbitals of Fe of CsFe_2Se_2 in the bi-collinear AFM state (see Fig. 4), we find that the five up-spin orbitals are almost filled and the five down-spin orbitals are nearly uniformly filled by half. This indicates that the crystal field splitting imposed by Se atoms is very small. As the Hund rule coupling is strong, this would lead to a large magnetic moment formed around each Fe atom, as found in our calculations. The formation of Fe magnetic moments is thus due to the Hund's rule coupling, which is a universal feature found in all the iron-pnictides [14, 15].

Further inspection of the charge distribution in real space shows that there is the covalence bond formed between the two nearest neighbor Fe and Se atoms, which is responsible for the next nearest neighbor Fe-Fe superexchange coupling J_2 . This superexchange is antiferromagnetic because the intermediated state associated with the hopping bridged by Se atom is a spin singlet. Thus we find the Se-bridged superexchange antiferromagnetic interaction between the next nearest neighbor Fe-Fe atoms in CsFe_2Se_2 and KFe_2Se_2 , which is again similar to the

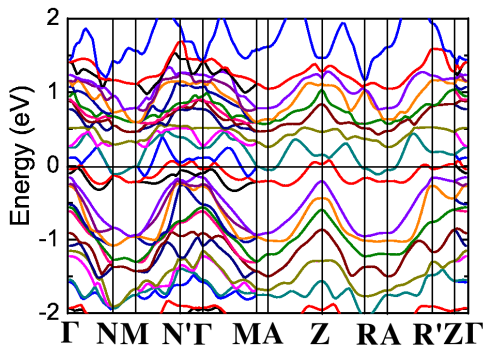


FIG. 6: (Color online) Electronic band structure of TlFe_2Se_2 in the bi-collinear-ordered antiferromagnetic state. The Brillouin zone is shown in Fig. 3(b). Notice that Γ -N(Γ -N') corresponds the parallel(antiparallel)-aligned moment line.

ones in all the iron pnictides [14, 15]. Nevertheless, there is a substantial difference between CsFe_2Se_2 (KFe_2Se_2) and the iron pnictides, regarding the next next nearest neighbor Fe-Fe exchange interaction J_3 .

Fig. 5 shows that the band formed by Se $4p$ orbitals is partially filled at the Fermi energy in CsFe_2Se_2 and KFe_2Se_2 . So there are itinerant $4p$ electrons at the Fermi energy involved in mediating the exchange interactions in CsFe_2Se_2 and KFe_2Se_2 . This may explain why the next next nearest neighbor superexchange coupling J_3 is large for CsFe_2Se_2 and KFe_2Se_2 due to an RKKY-like mechanism. In contrast, the band formed by As $4p$ orbitals is gapped at the Fermi energy in the iron pnictides [14, 15], correspondingly the next next nearest neighbor superexchange coupling J_3 is nearly zero.

A physical picture suggested in our study is thus that the Fe moments in CsFe_2 and KFe_2Se_2 are also partially mediated by partially delocalized Se $4p$ -band and the origin of J_3 exchange coupling may be well induced through an RKKY-like mechanism besides the Se-bridged superexchange antiferromagnetic interaction J_2 . Meanwhile, the exchange interactions J_2 and J_3 are in strong frustration competition, which is sensitively modulated by the Fe-Se bonding and related local environment, as we see from α -FeSe ($J_3 < I_2/2$) [8] to CsFe_2Se_2 and KFe_2Se_2 here ($J_3 > I_2/2$). By our calculation, it is clear that the magnetic order should be along the diagonal direction of the Fe-Fe square lattice for CsFe_2Se_2 and KFe_2Se_2 since J_3 is larger than $J_2/2$. However, it is also very likely that defects, vacancies, or other impurities would drive the bi-collinear antiferromagnetic order into an incommensurate spin order along the diagonal direction in CsFe_2Se_2 and KFe_2Se_2 , similar to the ones found in α -FeTe [18].

Although Tl is not an alkali metal element, our calculations show that the electronic and magnetic structures of TlFe_2Se_2 are overall quite similar to the ones of

CsFe_2Se_2 and KFe_2Se_2 . The electronic band structure and the Fermi surface of TlFe_2Se_2 in the nonmagnetic state are found by our calculations to be the same as the ones reported for TlFe_2Se_2 in Ref. 19. However, we find that the ground state of TlFe_2Se_2 is in the bi-collinear AFM order with a magnetic moment of $\sim 2.7\mu_B$ around each Fe atom rather than the square Neel AFM order reported in Ref. 19. The corresponding electronic band structure is shown in Fig. 6.

In conclusion, we have presented the results of the electronic band structure and magnetic properties of AFe_2Se_2 ($A=\text{K}, \text{Cs}, \text{or Tl}$) based on the first-principles electronic structure calculations. our studies show that the ground state of AFe_2Se_2 is a quasi-2-dimensional bi-collinear antiferromagnetic semimetal with a magnetic moment of $\sim 2.8\mu_B$ around each Fe atom. This bi-collinear antiferromagnetic state can be understood by the Hesenberg model with J_1 - J_2 - J_3 superexchange interactions.

This work is partially supported by National Natural Science Foundation of China and by National Program for Basic Research of MOST, China.

* Electronic address: zlu@ruc.edu.cn

† Electronic address: txiang@aphy.iphy.ac.cn

- [1] Y. Kamihara, T. Watanabe, M. Hirano, and H. Hosono, *J. Am. Chem. Soc.* **130**, 3296 (2008).
- [2] M. Rotter, M. Tegel, and D. Johrendt, *Phys. Rev. Lett.* **101**, 107006 (2008).
- [3] X.C.Wang, Q.Q. Liu, Y.X. Lv, W.B. Gao, L.X.Yang, R.C.Yu, F.Y.Li, and C.Q. Jin, *Solid State Commun.* **148**, 538 (2008).
- [4] F.-C. Hsu, *et al.*, *Proc. Natl. Acad. Sci.* **105**, 14262 (2008).
- [5] Jiangang Guo, *et al.*, *Phys. Rev. B* **82**, 180520(R) (2010).
- [6] A. Krzton-Maziopa, *et al.*, arXiv:1012.3637.
- [7] M. Fang, *et al.*, arXiv:1012.5236.
- [8] F. Ma *et al.*, *Phys. Rev. Lett.* **102**, 177003 (2009).
- [9] S.L. Li, *et al.*, *Phys. Rev. B* **79**, 054503 (2009).
- [10] P. Giannozzi, *et al.*, <http://www.quantum-espresso.org>.
- [11] J. P. Perdew, K. Burke, and M. Ernzerhof, *Phys. Rev. Lett.* **77**, 3865 (1996).
- [12] D. Vanderbilt, *Phys. Rev. B* **41**, 7892 (1990).
- [13] I.R. Shein and A.L. Ivanovskii, arXiv:1012.5164.
- [14] F. Ma, Z.Y. Lu, and T. Xiang, *Phys. Rev. B* **78**, 224517 (2008).
- [15] F. Ma, Z.Y. Lu, and T. Xiang, *Front. Phys. China*, **5(2)**, 150 (2010).
- [16] J. Ferrer, *Phys. Rev. B* **47**, 8769 (1993).
- [17] C. Fang, B. A. Bernevig, and J. Hu, *Europhys. Lett.* **86**, 67005 (2009).
- [18] W. Bao *et al.*, *Phys. Rev. Lett.* **102**, 247001 (2009).
- [19] L. Zhang and D.J. Singh, *Phys. Rev. B* **79**, 094528 (2009).